AIP | Journal of Applied Physics

ZnO nanorod/GaN light-emitting diodes: The origin of yellow and violet emission bands under reverse and forward bias

Xinyi Chen, Alan Man Ching Ng, Fang Fang, Yip Hang Ng, Aleksandra B Djurišić et al.

Citation: J. Appl. Phys. **110**, 094513 (2011); doi: 10.1063/1.3653835
View online: http://dx.doi.org/10.1063/1.3653835
View Table of Contents: http://jap.aip.org/resource/1/JAPIAU/v110/i9
Published by the American Institute of Physics.

ZnO nanorod/GaN light-emitting diodes: The origin of yellow and violet emission bands under reverse and forward bias

Xinyi Chen,[1] Alan Man Ching Ng,[1,2] Fang Fang,[1] Yip Hang Ng,[1] Aleksandra B Djurišić,[1,a)] Hoi Lam Tam,[3] Kok Wai Cheah,[3] Shangjr Gwo,[4] Wai Kin Chan,[5] Patrick Wai Keung Fong,[6] Hsian Fei Lui,[6] and Charles Surya[6]

[1]*Department of Physics, The University of Hong Kong, Pokfulam Road, Hong Kong, People's Republic of China*
[2]*Nanostructure Institute for Energy and Environmental Research, Division of Physical Sciences, South University of Science and Technology of China, Shenzhen, China*
[3]*Department of Physics, Hong Kong Baptist University, Waterloo Road, Kowloon Tong, Hong Kong*
[4]*Department of Physics, National Tsing-Hua University, Hsinchu 30013, Taiwan*
[5]*Department of Chemistry, The University of Hong Kong, Pokfulam Road, Hong Kong*
[6]*Department of Electronic and Information Engineering, Hong Kong Polytechnic University, Hung Hom, Kowloon, Hong Kong*

(Received 20 May 2011; accepted 20 September 2011; published online 9 November 2011)

ZnO nanorods have been prepared by electrodeposition under identical conditions on various p-GaN-based thin film structures. The devices exhibited lighting up under both forward and reverse biases, but the turn-on voltage and the emission color were strongly dependent on the p-GaN-based structure used. The origin of different luminescence peaks under forward and reverse bias has been studied by comparing the devices with and without ZnO and by photoluminescence and cathodoluminescence spectroscopy. We found that both yellow-orange emission under reverse bias and violet emission under forward bias, which are commonly attributed to ZnO, actually originate from the p-GaN substrate and/or surface/interface defects. While the absolute brightness of devices without InGaN multiple quantum wells was low, high brightness with luminance exceeding 10 000 cd/m^2 and tunable emission (from orange at 2.1 V to blue at 2.7 V, with nearly white emission with Commission internationale de l'éclairage (CIE) coordinates (0.30, 0.31) achieved at 2.5 V) was obtained for different devices containing InGaN multiple quantum wells. © *2011 American Institute of Physics*. [doi:10.1063/1.3653835]

I. INTRODUCTION

ZnO is a material of considerable interest for a variety of optoelectronic applications.[1] One of the attractive properties of ZnO is that it can be prepared by simple and low cost methods, so that it offers an attractive alternative for the development of cost-reduced light emitting diodes (LEDs). In recent years, in spite of progress made in achieving p-type ZnO, there has been increasing interest in ZnO based heterojunctions, in particular LEDs based on GaN/ZnO heterojunctions.[2–29] Although GaN-based technology is well developed, the use of ZnO could potentially lead to lower cost and higher brightness devices.

The majority of GaN/ZnO devices reported in the literature are based on p-GaN/n-ZnO material combination, although n-GaN/p-ZnO devices have also been reported.[23] However, very different behavior has been reported for p-GaN/n-ZnO devices even for similar device architectures, which makes it difficult to establish strategies for the improvement of device performance. For example, in addition to devices lighting up under forward bias, devices lighting up under reverse bias[4,8–10,12,13,28] have been reported. Also, a variety of the emission peaks at different wavelengths have been observed, including UV, UV-violet, violet-blue, green, yellow, and orange-red, with multiple peaks frequently present[11,14,18,19,22] which in some cases results in white emission.[21,28] These emissions have been attributed to different mechanisms in the literature. The assignment of the emission peaks in the electroluminescence (EL) spectra is typically performed on the basis of comparison with the photoluminescence (PL) spectra.[4,7] Such assignment is difficult when there are no corresponding peaks in the PL spectra, as in the case of commonly observed violet emission which falls between the PL peaks of ZnO and p-GaN. Furthermore, unlike ZnO, p-GaN substrates rarely exhibit significant PL emission in green-to-red spectral range. Consequently, yellow-orange defect emission is commonly attributed to the defect states in ZnO,[4,28] while UV-Violet emission which typically falls between the PL peaks of ZnO and GaN has been attributed to both ZnO (Ref. 24) and GaN (Ref. 17), with different reasons proposed to explain the peak shift.

In addition to controversies concerning the origins of emission peaks, in almost all cases EL is given in arbitrary units even though the light emission from p-ZnO/n-GaN based devices is frequently described as high brightness.[2,22,24] Thus, in majority of reports, there are no data available on absolute brightness or quantum efficiency of the devices. In those few cases, where efficiency was given, it was typically low (0.00005% (Ref. 6) and 0.06% (Ref. 29)). Obviously, significant improvements in the light emission intensity and efficiency are needed for practical applications.

a)Electronic mail: dalek@hku.hk.

These improvements could be achieved by improving the material quality as well as by optimizing the device architecture and improving our understanding on which factors contribute to the light emission in this type of devices.

Therefore, the objective of our study is twofold: to study the origin of different emission bands in heterojunction LEDs based on p-GaN/n-ZnO heterojunctions and to develop high brightness devices based on p-GaN/n-ZnO heterojunctions. To study the origin of the different emission bands, we prepared devices on different p-GaN based structures, both with ZnO and without ZnO (with different metal electrodes). The purpose of including the devices without ZnO is to investigate whether EL peaks different from those present in PL (since PL is commonly used for emission origin investigation) can be observed. Obtained results indicate that all the emission peaks (orange, yellow, blue under reverse bias, and violet under forward bias), originate from the p-GaN layer and/or GaN/ZnO interface since they can be observed in the absence of ZnO, as discussed in the Subsection III D. To improve the brightness of the devices, we have utilized a simple approach of growing ZnO nanostructures on a commercial group-III nitride-based LED wafer.[10,30] It has been shown that device architectures containing ZnO and InGaN multiple quantum wells (MQWs),[31–33] where dominant light emission peak originates from InGaN MQW,[31–33] can result in bright devices with low turn-on voltage (2.5 V).[31,32] Thus, we have employed a simple method of growing ZnO nanorods by electrodeposition on top of a commercial, unetched GaN-based LED wafer followed by the deposition of electrode onto ZnO, without any etching steps involved. Using such a simple process, high brightness devices have been achieved, as discussed in Subsection III E.

II. EXPERIMENTAL DETAILS

The p-GaN-based structures used are defined in Table I. QW1 and QW2 were obtained from Epistar Corporation, Taiwan. P1 samples were grown by metal organic chemical vapor deposition (MOCVD) on c-face sapphire substrates and annealed for dopant activation after the growth at Hong Kong Polytechnic University. P2 and P3 samples were obtained from TDI Oxford Instruments. The carrier/acceptor concentration in the samples was provided by the supplier of the samples and verified by electrochemical impedance spectroscopy (EIS) measurements.[34–36] EIS was used as a technique capable of providing information for carrier concentration for both nanorods[34] and thin films,[35] unlike Hall measurements which could be used only for thin films. EIS was performed in a three-electrode cell. The counter electrode was Pt sheet (1.5×1.5 cm^2) and reference electrode was standard Ag/AgCl electrode in 3 M KCl solution. The electrolyte used was carbonate propylene (0.1 M $LiClO_4$) and 0.1 M KCl for ZnO and p-GaN, respectively.[34,35] All EIS data were obtained using CH Instruments electrochemical workstation and the analysis was done by commercial software from CH Instruments. For ZnO, 20 mV sinusoidal signal was applied with constant dc bias, with frequency ranging from 500 kHz and 5 mHz.[34] For p-GaN, ac sinusoidal signal with 10 mV amplitude with constant dc bias and frequency ranging from 100 Hz to 500 kHz was used, and before the start and during the experiment cell was purged with argon gas.[35] The equivalent circuit consisted of a series resistance R_s and parallel connection of a capacitance and a constant phase element for ZnO, while for p-GaN equivalent circuit consisted of a series resistance R_s and parallel connection of a capacitance and a constant phase element in series with parallel resistance R_p. Carrier concentration was then determined by Mott-Schottky analysis. For ZnO nanorods, geometric approximation proposed in Ref. 34 was used, with the rod dimensions and density estimated from scanning electron microscopy images.

TABLE I. Labels and corresponding GaN structures.

Label	GaN structure
P1	p-GaN (550 nm, $p_{Hall} \sim 5 \times 10^{17}$ cm^{-3}, $p_{EIS} \sim 6.2 \times 10^{17}$ cm^{-3})/Mg:GaN, resistive, 550 nm/undoped-GaN, 2.2 μm/GaN nucleation layer, and 30 nm/sapphire
P2	p-GaN (4 μm, $N_a = 1\text{-}3 \times 10^{18}$ cm^{-3} and $p_{EIS} \sim 3.2 \times 10^{16}$ cm^{-3})/sapphire
P3	p-GaN (5 μm, $N_a = 5\text{-}8 \times 10^{17}$ cm^{-3} and $p_{EIS} \sim 5.0 \times 10^{17}$ cm^{-3})/sapphire
QW1	p-GaN (120-180 nm and $p_{EIS} \sim 1.1 \times 10^{18}$ cm^{-3})/InGaN MQWs/n-GaN/undoped-GaN/sapphire
QW2	p-GaN (222 nm, $N_a = 5\text{-}10 \times 10^{19}$ cm^{-3}, and $p_{EIS} \sim 1.2 \times 10^{18}$ cm^{-3})/InGaN MQWs/n-GaN/undoped-GaN/sapphire

Before use, the substrates were cleaned by sonicating in toluene, acetone, ethanol, and deionized water and then dried with nitrogen. A contact pad consisting of 30 nm Ni and 80 nm Au was deposited as a contact to p-GaN layer using AST Peva-500EL thermal evaporator. The contact was verified to be ohmic.[37] Ohmic contact in spite of the absence of post-deposition annealing likely occurred due to elevated sample holder temperature during deposition (~150-160 °C at the end of the Ni/Au deposition due to high source temperature, sample holder was not intentionally heated).

For electrodeposited ZnO nanorods, the solution for the nanorod growth was composed of 70 mg of zinc nitrate hydrate ($Zn(NO_3)_2 \cdot \times H_2O$, 99.999%, Aldrich) and 30 mg of hexamethylenetetramine (HMT, $C_6H_{12}N_4$, 99%, Aldrich) in 30 ml deionized water, and a two-electrode deposition setup was employed.[13] A platinum foil was used as the anode while the substrate was used as the cathode. The solution was heated up to 80 °C. A fixed current of 10 mA was first applied for 1 min and then a fixed current of 1 mA was applied for another 29 min. The sample was then sonicated for ~1 s in deionized water and then rinsed with deionized water and dried with nitrogen.

The morphology of the ZnO nanorods and film was studied by scanning electron microscopy (SEM, JEOL JSM-7001 F). Carrier concentration was determined by EIS.[34–36] Cathodoluminescence (CL) measurements were also performed using JEOL JSM-7001 F SEM equipped with a CL setup (Gatan, Mono CL). For PL measurements at room temperature and variable power, a HeCd laser (325 nm) was used as an excitation source and the spectra were collected using a PDA-512_USB (Control Development Inc) fiberoptic spectrometer. For variable temperature, PL spectra 337 nm nitrogen laser (20 Hz and 100 nW) was used as an excitation source, while a monochromator (Acton SpectraPro 500i)

with Peltier-cooled photomultiplier detector (Hamamatsu R636-10) was used to collect the emission spectra.

To complete nanorod devices, spin-on-glass (SOG, Futurex, Inc.) was used to prevent the short circuit.[10,12,13] SOG was spin-coated at 3000 rpm for 40 s and then annealed at 200 °C for 1 min. Devices with poly(methyl methacrylate) as the insulating layer[3] were also prepared. 2% PMMA (molecular weight: 950 000, MicroChem.) solution in chlorobenzene was spin-coated at 4000 rpm for 45 s and baked at 200 °C for 1 min. The excess PMMA from the tops of the nanorods was removed using oxygen plasma (100 W for 15 s) prior to metal contact deposition. ITO/ZnO nanorods+SOG/Ag devices were used to verify that Ag forms an ohmic contact with ZnO. The top metal electrode (Ag, 200 nm) was deposited through a shadow mask (circles with 1 mm radius) by thermal evaporation using AST Peva-500EL thermal evaporator. The same deposition method was used for the deposition of different metal contacts (Ag, Al, Cu, and Mg (100 nm):Ag(50 nm)) directly on p-GaN. Schematic diagram of the LED devices is shown in Figure 1. To compare the performance of nanorod based devices, LEDs with ZnO film were also prepared. ZnO film was deposited from ZnO pellets (Lesker, 99.9%) in high vacuum using AST Peva-400ES e-beam evaporator at a substrate temperature of 300 °C. EL and I-V measurements were performed using a Keithley 2400 source meter to provide a fixed voltage bias, and the emission spectra were collected using a monochromator (Acton SpectraPro 500i) with Peltier-cooled photomultiplier detector (Hamamatsu R636-10). Luminance was measured using Minolta Luminance Meter LS-100. The emission power was also verified using a Newport 1830-C optical power meter equipped with a 818-UV detector probe (for higher bias voltages where only a narrow blue emission peak is observed). External quantum efficiency (EQE) was calculated from measured optical power at different bias conditions.

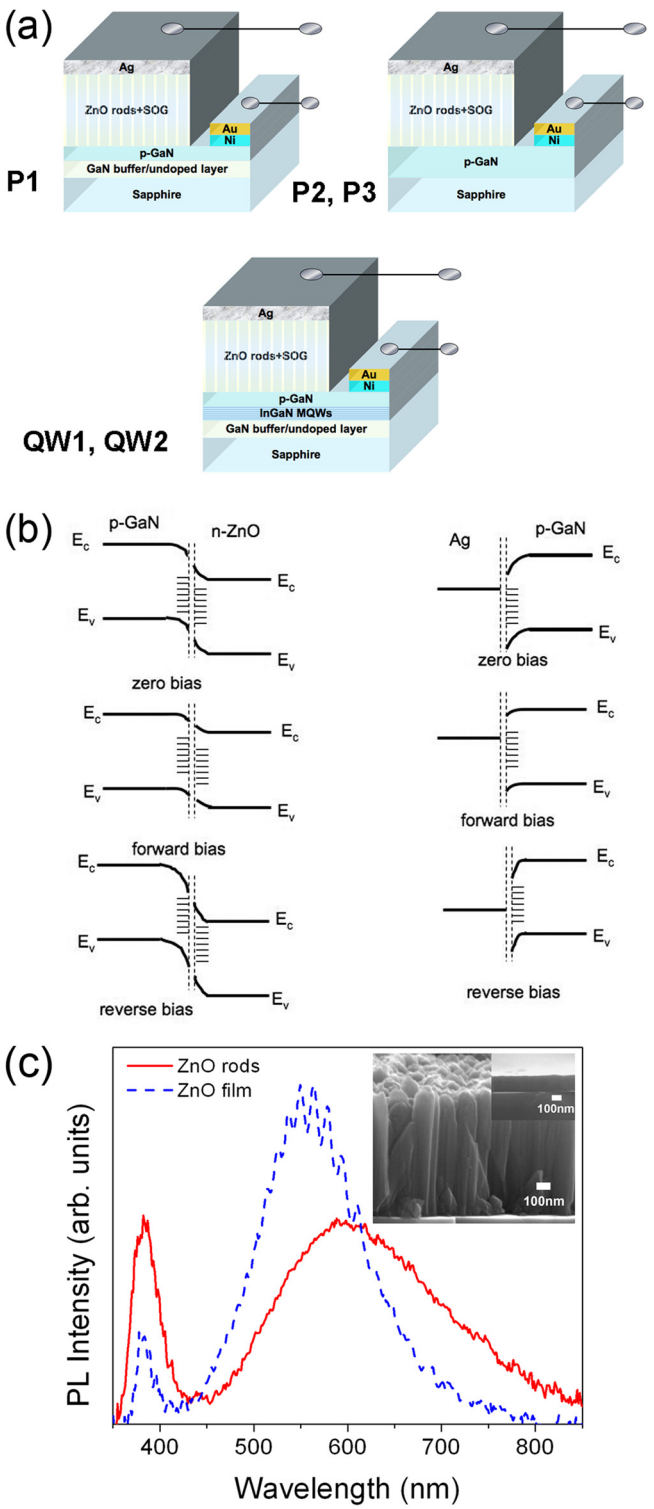

FIG. 1. (Color online) (a) Schematic diagrams of different devices with ZnO nanorods. (b) Schematic energy band diagrams of the GaN/ZnO devices (left) and GaN/Ag devices (right). (c) PL spectra of ZnO nanorods and film. The inset shows the cross section SEM of ZnO nanorods and film.

III. RESULTS AND DISCUSSION

We have investigated the origin of different emission bands in ZnO LEDs by using various GaN-based substrates, as summarized in Table I. Typical device schematic diagrams and the corresponding energy band diagram for a p-GaN/n-ZnO type II heterojunction is shown in Fig. 1. It should be noted that the device architecture for devices on QW1 and QW2 substrates is complex, since the devices contain more than one p-n junction. The contact geometry has some similarity with the light-emitting transistors,[38–40] which also include devices with layered electron and hole transporting layers with two contacts deposited on the top of the device.[40] While our devices do not have gate electrode for additional modulation of the charge injection and light emission, it has been shown that the light emission in a light emitting transistor can occur at certain drain-source bias voltages independent on the gate voltage.[38] Thus, complex device architectures can have practical relevance even though they are more complicated to understand compared to simple p-n junctions. It should also be noted that the top p-GaN layer in QW1 and QW2 devices is very thin (of the order 100-200 nm), so that at larger bias, the current spread is expected to include MQW area. The device performance parameters are summarized in Table II. On all substrates, dense arrays of ZnO nanorods with good perpendicular orientation were obtained, as shown in Fig. 1(c). Both ZnO films and nanorods exhibited UV emission as well as visible emission attributed to native defects. The position of the native defect emission was different in the nanorods and films, indicating different types and concentrations of defects which will be discussed in more detail in the following. The nanorod

arrays and films also exhibited similar carrier concentrations, $4.4 \times 10^{19}\,cm^{-3}$ and $2.9 \times 10^{19}\,cm^{-3}$, respectively.

A. I-V curves

The I-V curves of P1-P3 devices, shown in Fig. 2, are consistent with the presence of tunneling mechanisms and show a shape resembling the backward diode.[10,12,13,41] Similar I-V curve shapes can also be observed for QW1 and QW2 devices.[37] The contacts have been verified to be ohmic,[37] as illustrated in the inset of Fig. 2(b). Backward diode shape of the I-V curve is consistent with the fact that carrier concentration in ZnO is significantly higher compared to hole concentration in p-GaN layers.[41] While the I-V curve shapes are similar, there are differences in the magnitude of current for the same bias voltage among different samples, which can likely be attributed to differences in carrier concentrations and/or differences in surface/interface defects due to different properties of P1-P3, QW1, and QW2. Since the I-V curves do not follow the trends of carrier concentrations in the substrate, we can conclude that surface/interfacial defects in p-GaN layer have a more significant effect on the obtained I-V curves. To investigate the mechanisms

TABLE II. Summary of device performance parameters. For peak wavelengths in devices exhibiting peak shifts, bias voltage is specified in the brackets. V_T denotes turn-on voltage, F denotes forward bias, and R denotes reverse bias. All devices with ZnO are with PMMA, except QW1-ZnO which is with SOG.

Devices	V_T,F (V)	V_T, R (V)	F emission peak wavelength (nm)	R emission peak wavelength (nm)
P1-Ag	—	3	—	~566 (3-6 V) ~380, 452, 566 (8-16 V)
P2-Ag	12	7	424	620 (8-16 V) 604 (18-20 V) 586 (22 V), 576 (24 V)
P3-Ag	15	8	424	650 (8-10 V) 618 (12 V), 602 (14 V)386, 578 (16 V)
P1-ZnO	—	10	—	569
P2-ZnO	13	10	436, 690 (13 V) 430, 622 (14 V) 416 (15 V) 406 (16 V) 404 (17 V) 400 (18 V)	~622 (10-14 V) 374, 622 (15-17 V)
P3-ZnO	15	12	438 (15 V) 418 (18 V) 390 (21 V)	648 (12 V), 664 (15 V) 428, 632 (16 V) 428, 622 (17 V) 426, 618 (18 V) 426, 606 (19 V) 390, 590 (20 V)
QW1-Ag	15	2	430 (40 V)	474, 610 (2.1 V) 474, 604 (2.2 V) 472, 590 (2.3 V) 472, 588 (2.4 V) 474, 574 (2.5 V) 474 (2.6 V)
QW2-Ag	26	2.2	456 (40 V)	460
QW1-ZnO	50	2	390 (60 V)	478, 622 (2.1 V) 474, 610 (2.2 V) 474, 596 (2.3 V) 474, 586 (2.4 V) 474, 578 (2.5 V) 474, 572 (2.6 V) 476, 568 (2.7 V)
QW2-ZnO	18	2.3	458 (40 V)	466

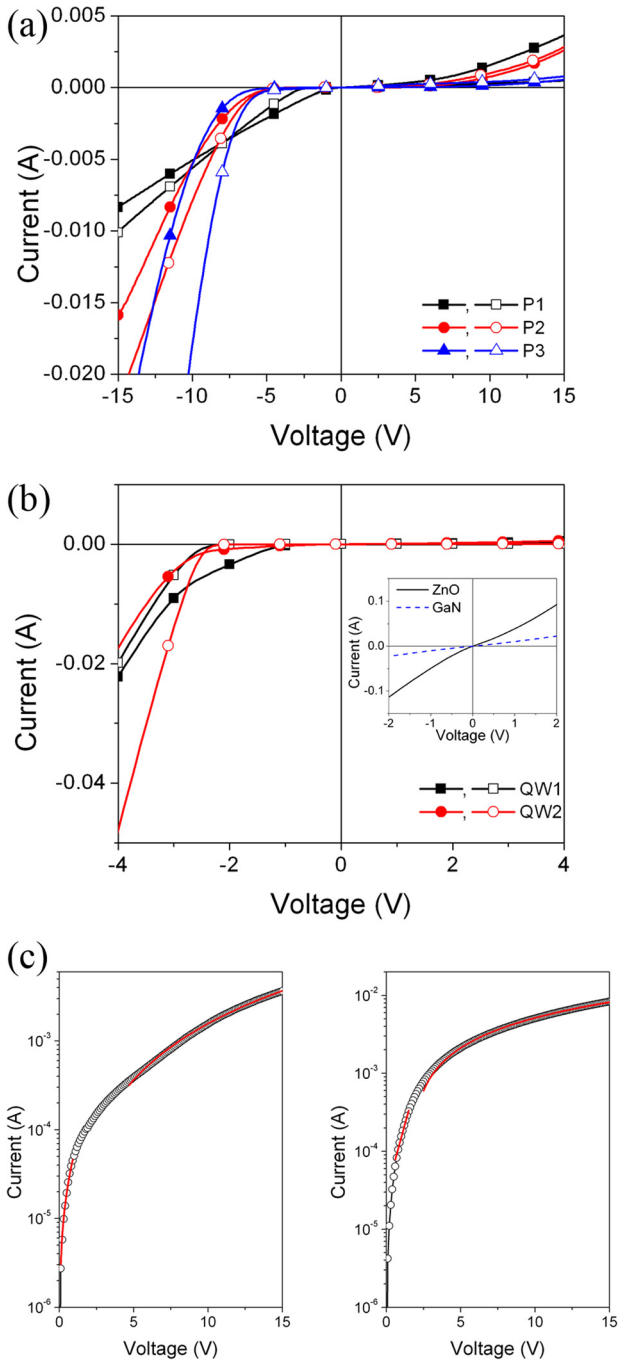

FIG. 2. (Color online) I-V curves of (a) P1, P2, P3 devices with ZnO (closed symbols), and Ag (open symbols) (b) QW1 and QW2 devices ZnO (closed symbols) and Ag (open symbols), the inset shows the ohmic contact check for ZnO (ITO/ZnO nanorods/Ag) and p-GaN (p-GaN-Ni/Au); fitting of the I-V curve of P1-ZnO device for (c) forward bias and (d) reverse bias.

involved in charge transport in our devices, I-V curves were fitted. Obtained results are shown in Fig. 2(c) for ZnO-P1 device (selected as the best performing simple heterojunction device with ZnO). Under forward bias, at lower voltages ($0.1\,V < V < 0.9\,V$), the current can be fitted with $I = I_s[\exp(qV/nkT) - 1]$, where n is the ideality factor and I_s is the reverse saturation current.[41,42] Obtained value of the ideality factor is large ($n = 32.7$), which is not entirely unexpected for junctions involving wide band gap materials.[7,42] Large ideality factors have been previously attributed to the space-charge limited conduction, deep-level assisted tunneling, and parasitic rectifying junctions.[42] At higher forward bias ($4.5\,V < V < 15\,V$), the I-V curve could be described with $I \sim V^b$, where $b = 2.1$, close to the $I \sim V^2$ relationship common for wide band gap materials.[6] Under reverse bias, large current has been observed. n-ZnO/p-GaN heterojunction devices without intrinsic or insulating layers frequently show leaky I-V curves[6,9,10,14,17,29] in agreement with large currents under reverse bias observed in our work. Large leakage current was previously attributed to Pool-Frenkel effect.[32] However, Pool-Frenkel equation did not result in a good fit of the obtained I-V curves. On the other hand, good fit has been obtained in the range from $-0.6\,V$ to $-1.5\,V$ using a backward diode equation $I \approx C_5 \exp(|V|/C_6)$.[41] At higher reverse bias voltages ($> -2.5\,V$), linear I-V dependence is obtained. In that range, the current is larger so that the series resistance of the device likely contributes to the observed linear dependence.

B. Performance under reverse bias

Light emission under reverse bias has been previously reported in n-ZnO nanorod/p-GaN LEDs.[4,12] Lighting up under both forward and reverse bias has also been reported for p-GaN/n-ZnO (Refs. 8, 10, 13, and 28) and p-GaN/ZnO:SiO_2/ZnO devices.[9] Similar behavior, i.e., lighting up under both forward and reverse bias was observed in ZnO/p^+ Si heterojunctions, with UV emission at ~385 nm from ZnO under reverse bias attributed to tunneling.[43] All the investigated devices exhibited light emission under reverse bias.[37] The obtained emission spectra for P1, P2, and P3 devices are shown in Fig. 3.

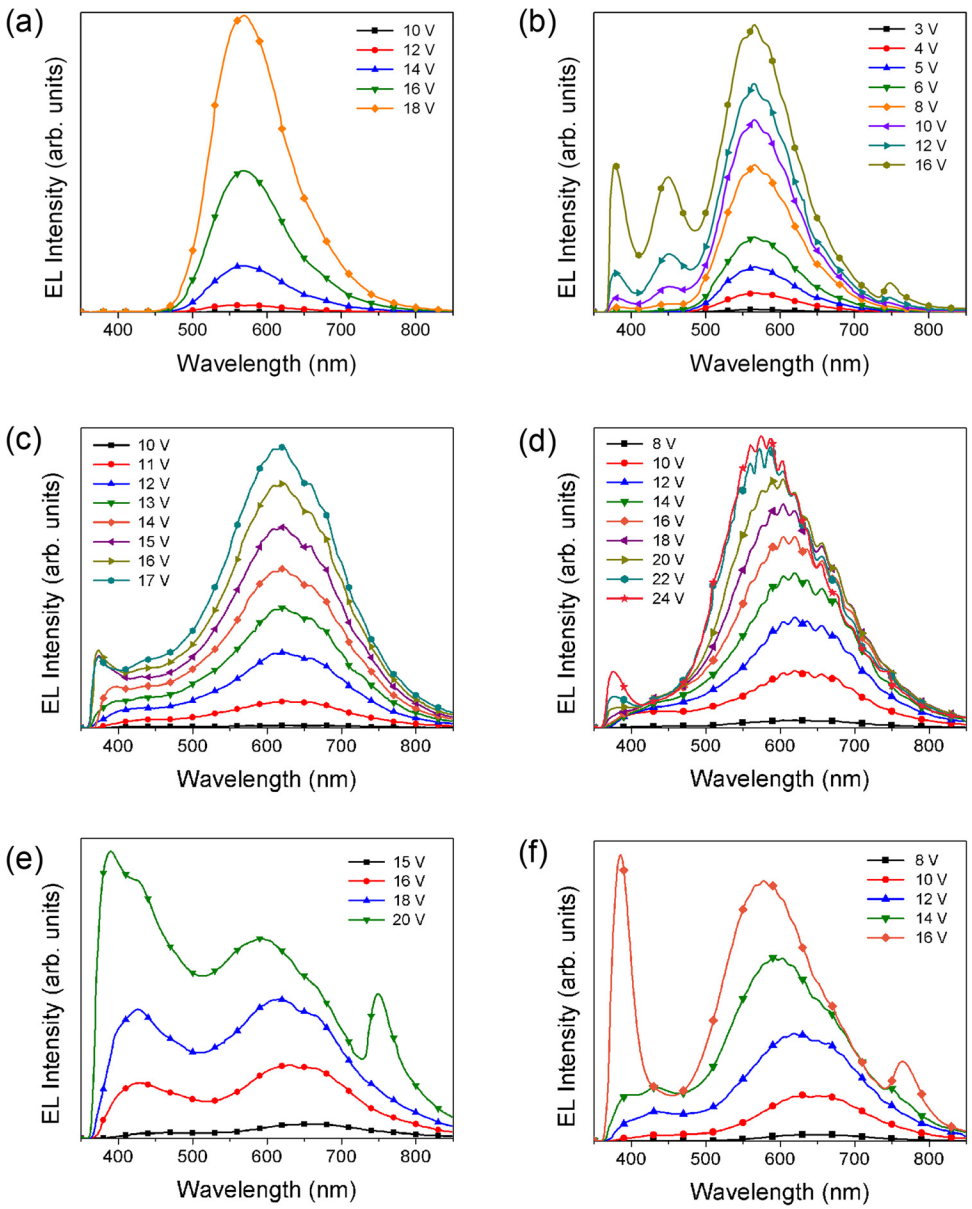

FIG. 3. (Color online) Electroluminescence spectra under different reverse bias voltages for devices with ZnO (PMMA) and Ag, respectively, on (a) and (b) P1, (c) and (d) P2, and (e) and (f) P3 substrates.

To examine whether light emission occurs from ZnO or from p-GaN, devices with a Ag metal contact are also included in addition to the devices with ZnO. Different devices have different turn-on voltages, so the bias voltages have been selected in such a way to clearly show the evolution of the shape of the spectra with increasing bias voltage. We can observe that the emission peaks which can occur under reverse bias are yellow/orange emission, blue emission, and UV emission. The broad long wavelength emission is typically attributed to the defect emission in ZnO based on comparisons with the PL spectra[4,14] since ZnO commonly exhibits broad visible emissions due to native defects.[44] However, while the exact peak positions for yellow/orange emission, blue emission, and UV EL emission differ for devices with ZnO and with Ag, we can clearly observe that emissions absent in the PL spectrum of P1-P3 (Ref. 37) can occur in absence of ZnO. Thus, the presence of yellow-orange emission in the PL spectrum of ZnO does not necessarily imply that yellow-orange EL emission originates from ZnO, and the differences in the peak positions likely originate from different energy level alignment across the interface and consequently involvement of different defect states. The origin of the emission peaks is discussed in more detail in Subsection III D.

There are two possible mechanisms to explain emission under reverse bias, reverse breakdown,[9] and tunneling across the interface.[4,8,10,12,13,28] The presence of a UV emission peak at ~365 nm corresponding to the band gap energy of GaN (~365 nm) which occurred at higher reverse bias voltages (>12.5 V) was attributed to avalanche breakdown due to strong electric field.[9] In some of the devices, blue emission from p-GaN can also be observed, and it decreases with increasing bias voltage while UV emission increases. Unlike avalanche breakdown which occurs at larger reverse bias voltages, tunneling can occur at smaller reverse bias. The tunneling is expected to occur due to the large energy band offset at p-GaN/n-ZnO interface.[4,8,10,12,13,28,45–47] The yellow (or orange yellow) emission appears at relatively low bias voltages, so that it likely occurs due to tunneling. Tunneling phenomena in III-nitride heterojunctions have been previously observed for different material combinations.[48–51] Furthermore, since the lattice mismatch between GaN and ZnO is higher than 1%, interface states are expected to significantly affect the current flow across the junction and severely limit the injection of the minority carriers.[52] Thus, significant current transport mechanisms in these devices are expected to involve tunneling and recombination at the interface,[52] and the tunneling likely involves the defect states at the interface, as illustrated in Fig. 1(b). The involvement of the interfacial states is also consistent with the observed I-V curves.

To further investigate the behavior of the light emission under reverse bias, we have prepared devices on QW1 with different ZnO (nanorods and films) and different metal contacts (metals expected to result in a Schottky contact to p-GaN have been selected, such as Ag, Al, Cu, and Mg:Ag).[37] Obtained emission spectra are shown in Fig. 4. The I-V curves of all devices had similar shape under reverse bias, while device with ZnO film had higher current under forward bias compared to other devices.[37] The ZnO nanorods and film obviously have different types and concentrations of native defects (see PL spectra in Fig. 1(c)), which is likely the reason for the observed difference. Depending on the type of material, small differences in the turn-on voltage and the position of the lower energy peak can be observed. However, in all the devices, we can observe the same trends, i.e., at lower voltages, the emission is dominated by a broad orange peak which exhibits blue shift and decreasing amplitude with increasing bias voltage, so that at higher biases, the spectrum

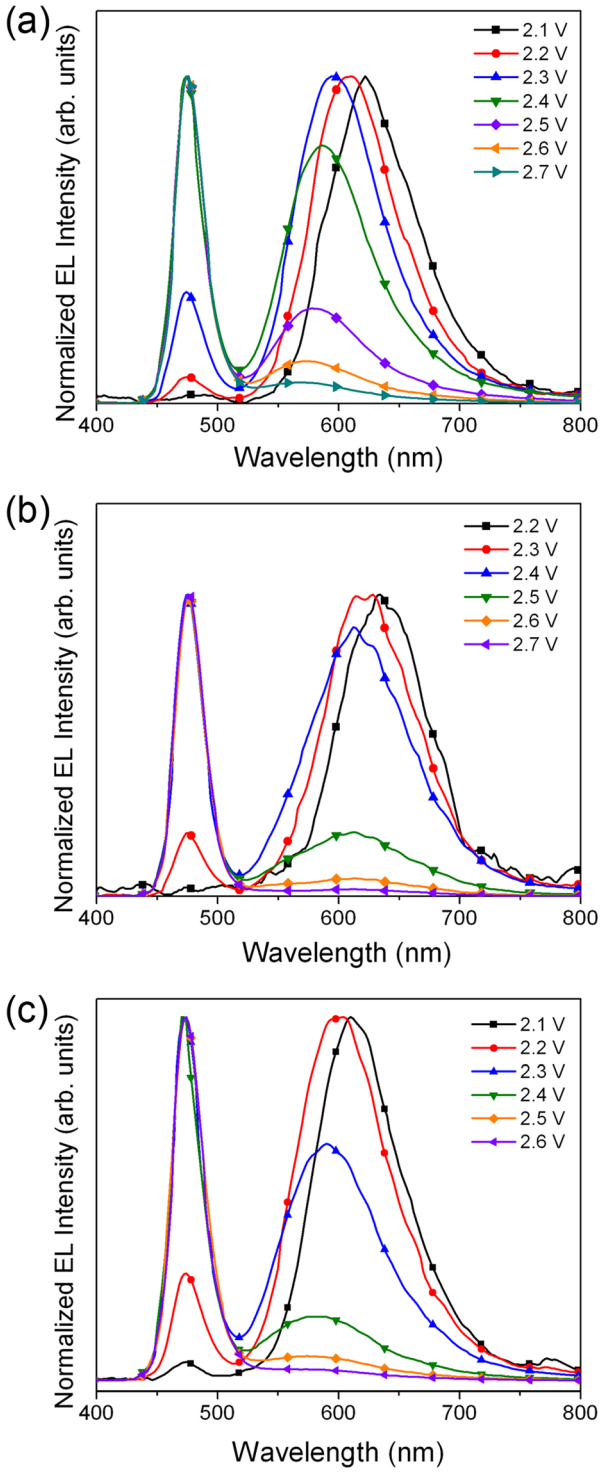

FIG. 4. (Color online) Electroluminescence spectra under different reverse bias voltages of the devices on QW1 substrates with (a) electrodeposited ZnO nanorods, (b) e-beam evaporated ZnO film, and (c) Ag.

is dominated by InGaN MQW emission at 475 nm. From the emission position and its high intensity, other origins of this emission are unlikely. Since the bias voltages are low (2-4 V) and no band edge peak of GaN is observed, the mechanism likely involves tunneling, same as in the devices without MQW structures. It should also be noted that in the case of ZnO film, the position of the broad orange EL emission peak does not match the position of defect emission in the film PL spectrum, indicating that this emission likely does not originate from defects in the ZnO film.

In all the devices, (P1, P2, P3, QW1, and QW2), all the emission peaks can be observed in the absence of ZnO (but exact peak position shows some difference depending on the material used).[37] Therefore, they obviously originate from p-GaN-based multilayer structure (or interface states). The exact origin of different transitions is discussed in detail in Subsection III D.

C. Performance under forward bias

Under forward bias, the devices typically exhibited UV-violet emission. This emission occurred at significantly higher voltage and lower brightness compared to the emission under reverse bias (possibly due to unfavorable energy band alignment across the interface). In some devices (on P1 and QW1), no emission under forward bias was observed for biases up to ~ 50 V, although in case of QW1, weak forward emission can be observed at higher voltages. Some differences in the I-V curves, turn-on voltages, and luminance have been observed in devices with ZnO nanorods and different insulating layers, SOG and PMMA. However, the EL spectra exhibited similar trends with increasing bias voltage.[37] The obtained EL spectra under forward bias for P1, P2, and P3 devices are shown in Fig. 5. It can be observed that the position of the emission peak is blue-shifted compared to ZnO emission and red-shifted compared to typical blue p-GaN emission, in agreement with the literature.[2,3,5,10,17,20,23,27] Similar UV-violet emission peak is also observed in devices on QW1 and QW2 substrates, as shown in Fig. 6. However, the fact that this emission occurs in the absence of ZnO, clearly indicates that it likely originates from p-GaN structures, and it likely involves defect/interface states. The width and exact peak position are contact material and p-GaN structure dependent, with broader peaks observed for metal contacts compared to ZnO/GaN, which can likely be attributed to the differences in the energy level alignment across the interface and involvement of different defect energy levels. Both p-GaN and ZnO have a rich defect chemistry and a number of energy levels within the gap is expected for both materials, resulting in complex emission behavior. Furthermore, due to higher carrier concentration in ZnO, as well as higher mobility of electrons compared to holes, under forward bias recombination would be expected to occur on the p-GaN side of the junction. The exact origin of this emission is discussed in Subsection III D.

D. The origin of the emission peaks

From the fact that both yellow-orange emissions and violet emissions are observable in the devices without ZnO (devices containing only GaN and metal contacts), they likely originate from p-GaN structures used. Although in principle, it could be possible that devices with ZnO exhibit emission in the same spectral range from ZnO, while devices without ZnO exhibit emission from GaN, two types of devices behave in a very similar way which indicates that emission most likely originates from GaN. Furthermore, yellow emission under reverse bias was previously observed from devices where ZnO exibited green rather than yellow defect luminescence.[12] Therefore, it is likely that the observed emissions originate from p-GaN. To investigate the properties of p-GaN structures used in more detail, we performed variable temperature PL measurements, variable power PL measurements, and CL measurements, and the obtained results are shown in Figs. 7–9, respectively, (only P2 is shown, since P2 and P3 are from the same supplier and have similar properties). CL from ZnO nanorods on P1 is also shown in Fig. 9(c). We can observe that in low temperature PL spectra, in addition to GaN band-to-band transition at $\sim$365 nm, there are obvious transitions in the range $\sim$370-400, in addition to the blue emission from p-GaN in P1 and InGaN MQWs in QW1 and QW2. In variable power PL spectra, the yellow emission is more prominent at low excitation powers for QW1 and QW2 samples. However, for P1 and P2, there is no significant signal in the yellow-orange range. No signal in this spectral range was obtained for CL measurements as well, while CL has shown additional peaks in the UV-violet region, similar to low temperature PL spectra.

Thus, it should be noted that yellow emission is only clearly observed in PL and CL spectra of QW1 and QW2, in spite of the presence of prominent yellow-orange emissions under reverse bias in P1, P2, and P3 devices (including devices without ZnO). One possibility is that this transition occurs due to interface states, which would be expected for a heterojunction with lattice mismatch exceeding 1%.[52] Furthermore, low energy emission band (1.9-2.7 eV) observed in nitride tunneling diodes was attributed to tunneling and found to be related to the high electric field strength.[49] Thus, under reverse bias, tunneling of the electrons occurs from p-GaN to ZnO resulting in the appearance of holes in the p-GaN. At the same time, the electron injection into p-GaN is expected to be more efficient than the injection of holes into ZnO, and consequently recombination would occur on the p-GaN side of the junction. Indeed, yellow emission in ZnO/GaN LEDs has been previously attributed to GaN lattice defects[11] and recombination involving deep acceptors. Concerning the difference in peak position between yellow and orange-red emission, this has been attributed to the transition involving deep acceptors (yellow) and transitions involving deep donors and deep acceptors (red).[28] For different materials in contact with p-GaN and for various p-GaN structures, changes in the energy level alignment across the interface would be expected, which would affect contributions of individual defect levels to the emission spectrum.

Concerning the origin of the violet emission under forward bias, it was attributed to different origins in the literature, such as radiative recombination in ZnO,[24] different contributions of band edge emissions of GaN and ZnO (Refs. 2 and 3) and interfacial recombinations,[2] recombination on defects in

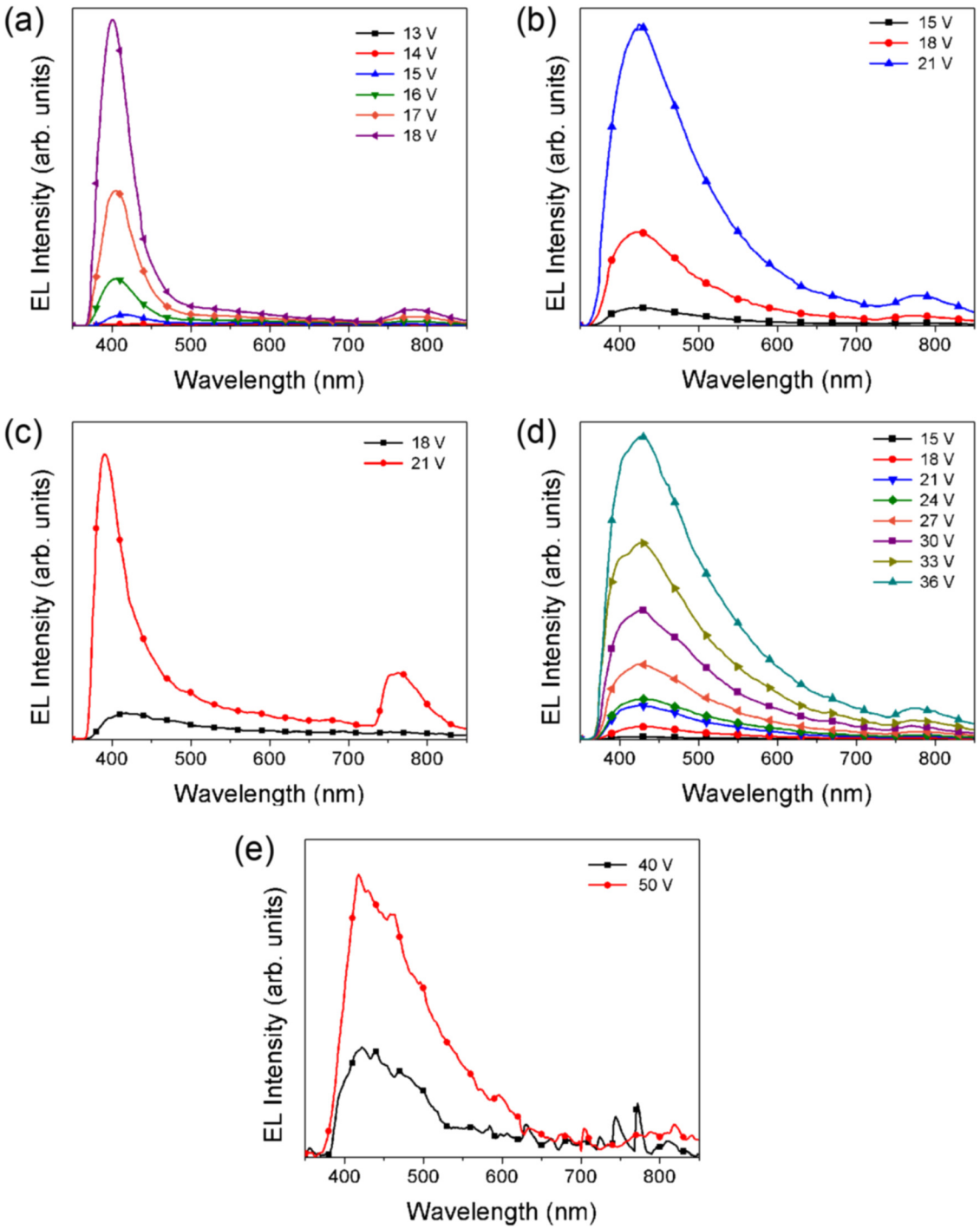

FIG. 5. (Color online) Electroluminescence spectra under different forward bias voltages for devices with ZnO (PMMA) and Ag, respectively, on (a) and (b) P2 and (c) and (d) P3. (e) ZnO (SOG) on P1.

p-GaN,[17] shift due to the energy band offsets in n-GaN/p-ZnO heterojunction,[23] as well as the presence of interfacial layer resulting in charge accumulation and bandgap renormalization.[27] Similar to yellow-orange emission, from the presence of this emission in the absence of ZnO, violet emission likely originates from p-GaN structures. In low temperature PL spectra and CL spectra, we can indeed observe additional peaks compared to room temperature PL spectra. A number of different defect levels has been demonstrated in GaN Schottky and p^+-n diodes.[53] Furthermore, it was proposed that in GaN, there is a deep quasi-continuous density-of-states distribution.[54] The abundance of defect states in p-GaN would consequently result in the appearance of a broad violet peak different from the usual blue emission. This emission likely involves both shallow and deep Mg acceptor levels.[15] The abundance of defect levels in GaN (Refs. 53 and 54) is also consistent with small differences in peak positions for different device architectures (GaN samples and ZnO or metal electrode), since small differences in the energy level alignment across the interface would result in the involvement of different defect states in the emission and consequently peak shift.

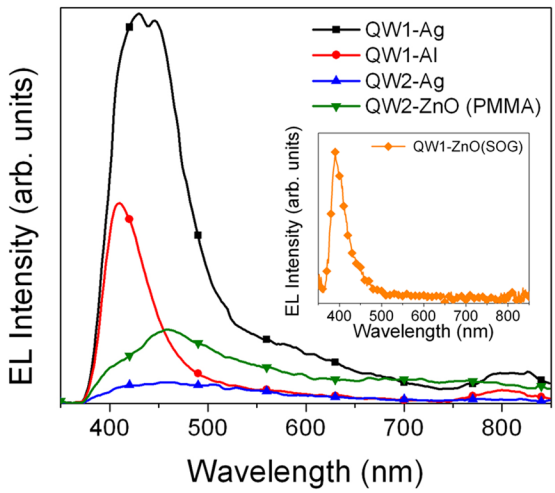

FIG. 6. (Color online) EL spectra under forward bias of 40 V for devices with ZnO and Ag on QW2 and Al and Ag on QW1. The inset shows EL spectrum under forward bias of 60 V for device with ZnO on QW1, which lights up at higher bias.

E. High brightness LEDs

The brightness of p-GaN/n-ZnO heterojunction devices is rarely reported (EL spectra are typically given in arbitrary units), but from the shape of the spectra and photographs of the devices, it can be deduced that the brightness is not high. The reported efficiency of the devices was typically very low,[6] below 0.1%.[6,29] The brightness that we have obtained from a simple p-GaN/n-ZnO heterojunction (P1) is of the order of tens of cd/m^2. On the other hand, devices on QW1 and QW2 exhibited significantly brighter emission under reverse bias.

For QW1 substrates which exhibit more prominent yellow defect emission (Fig. 8), we observe a change in the emission spectra with increasing bias voltage (as shown in Fig. 4), and in the case of devices with ZnO nanorods, we can observe white emission with Commission internationale de l'éclairage (CIE) coordinates (0.30, 0.31) at a reverse bias of 2.5 V. However, for QW2 devices, only blue emission from InGaN MQW structure is observed under reverse bias. This also confirms the important role of defect states in the shape of the emission spectra. The obtained results for the luminance of the devices with ZnO and Ag on QW1 and QW2 substrates are shown in Fig. 10. For QW1 substrates, the highest luminance is observed in devices with ZnO nanorods, and luminance for all the devices with the exception of those with Al contact is relatively high (several thousand cd/m^2 at a bias of − 4 V), as shown in Fig. 10(a). In addition

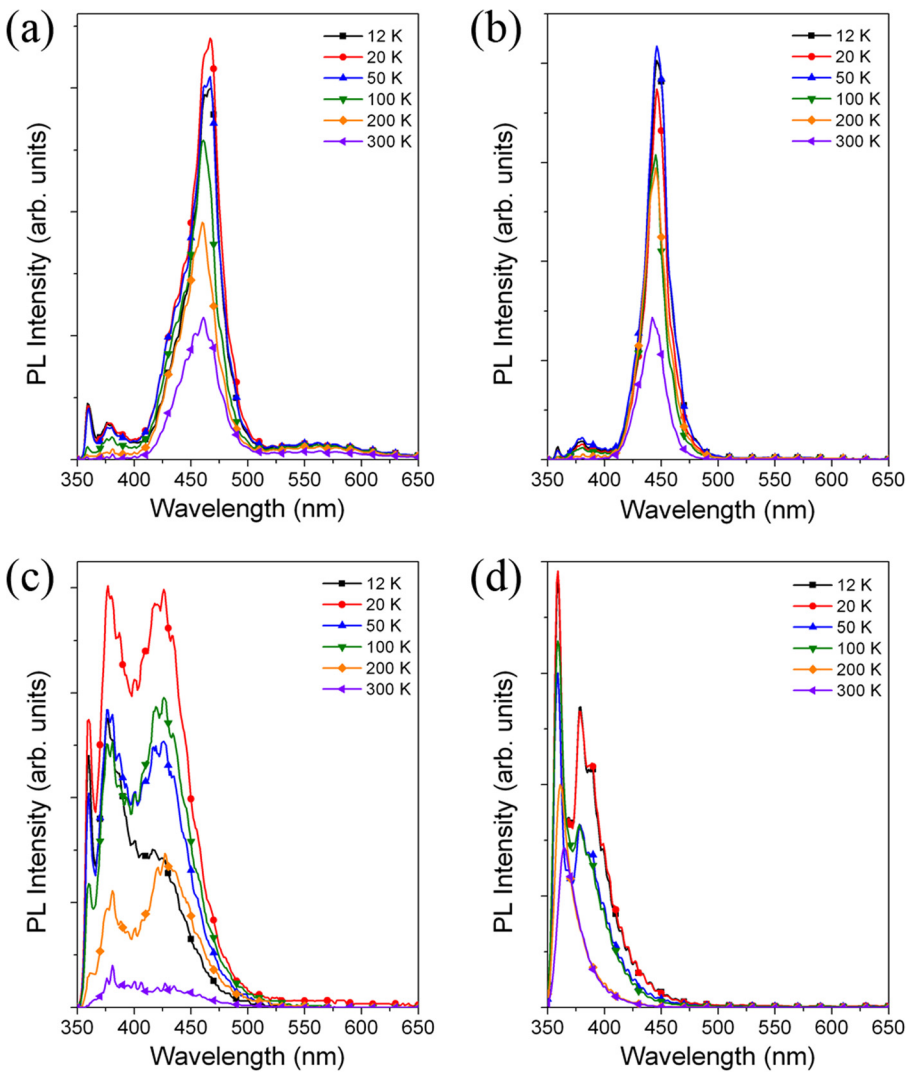

FIG. 7. (Color online) Variable temperature PL spectra of (a) QW1, (b) QW2, (c) P1, and (d) P2.

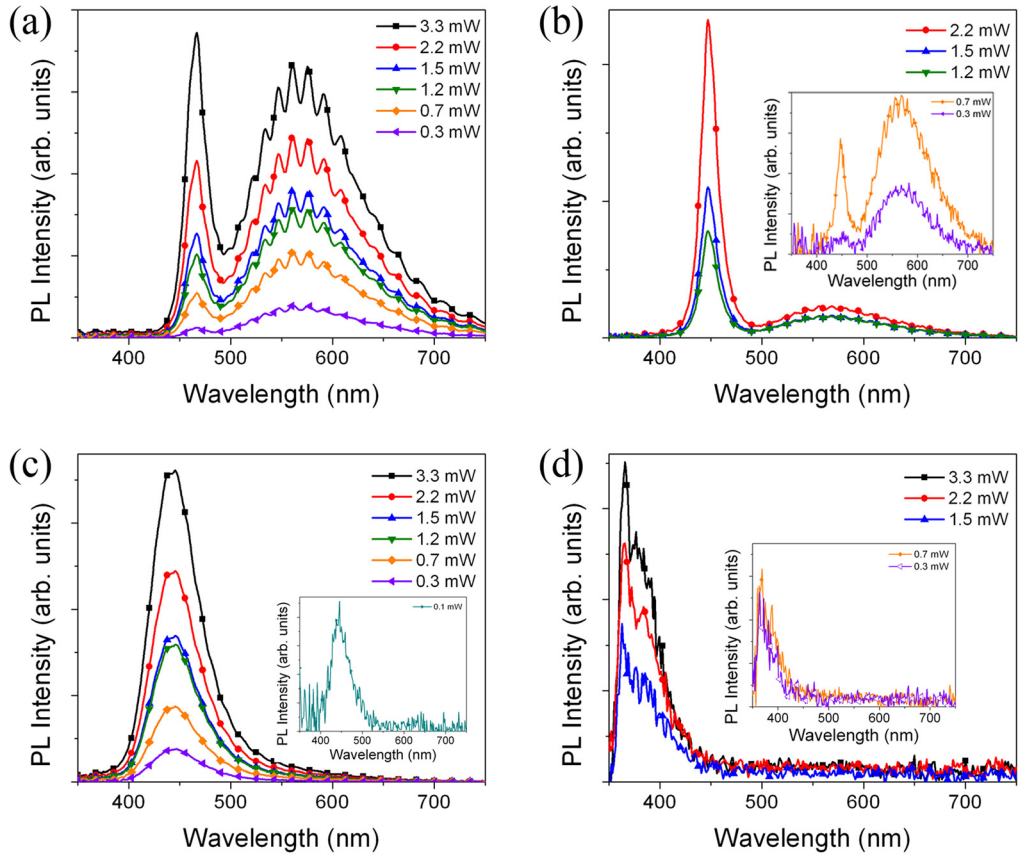

FIG. 8. (Color online) Variable power PL spectra of (a) QW1, (b) QW2, (c) P1, and (d) P2.

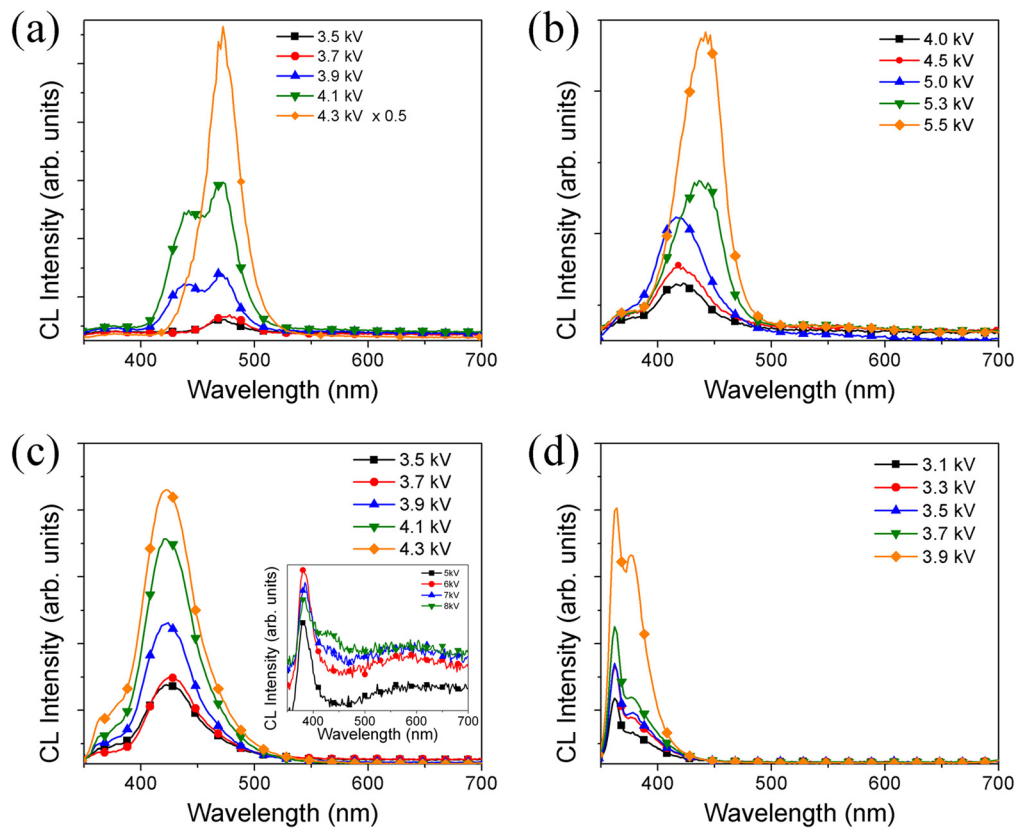

FIG. 9. (Color online) CL spectra of (a) QW1, (b) QW2, (c) P1 (the inset shows CL spectra of ZnO/P1 structure), and (d) P2.

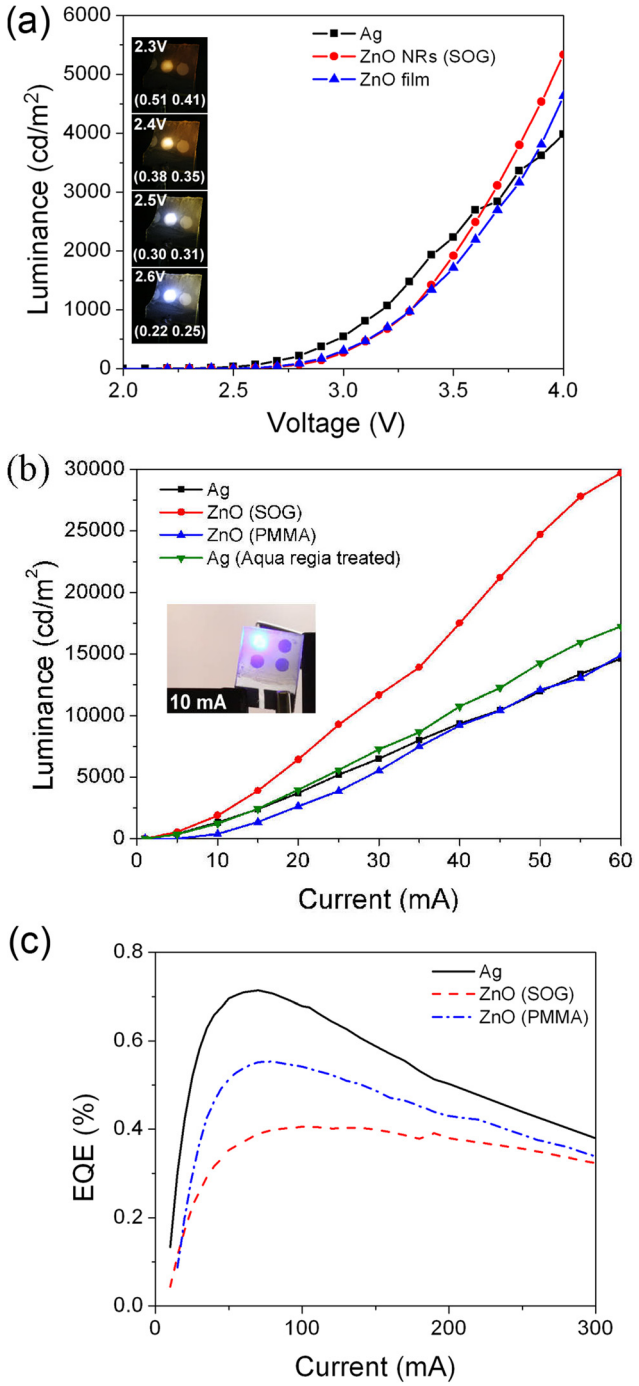

FIG. 10. (Color online) (a) L-V curves of devices on QW1 (b) L-I curves of devices on QW2. The insets show device photos. (c) EQE vs. bias current for QW2 devices with ZnO and Ag.

to luminance measurements, we have also measured emitted optical power from the devices and obtained 0.18 mW (3.94 V and 20 mA) for ZnO nanorod devices and 0.14 mW (3.91 V and 30 mA) for ZnO film devices.

For devices on QW2, higher luminance values were observed compared to QW1 substrates (at the same bias current, the obtained luminance for ZnO (SOG) device is ~ 2 times higher). In the case of Ag contact (with and without surface cleaning with aqua regia,[55] to investigate whether surface condition of p-GaN has an influence on the emission behavior), higher currents are observed for the same bias voltage above the turn-on voltage of ~ 2.0 V. Thus, to compare the brigthness of devices with ZnO and Ag contacts, current-driving instead of voltage-driving was performed and the obtained results are shown in Fig. 10(b). The highest brightness is obtained for device with ZnO nanorods and SOG insulator, exceeding 10 000 cd/m^2 for 30 mA current bias. The devices appear very bright even under ambient illumination. The reasons for higher luminance in case of SOG compared to PMMA are not fully clear, but they likely originate from differences in passivating surface defects in ZnO nanorods for these two materials. The external quantum efficiency of the devices is shown at Fig. 10(c). It can be observed that the devices with PMMA exhibit higher efficiency compared to SOG, while for Ag, higher efficiency is observed compared to ZnO. However, devices with SOG exhibit the smallest efficiency droop with increasing bias current. For both SOG and PMMA devices, achieved efficiencies are much higher compared to previous reports on heterojunction LEDs based on n-ZnO/p-GaN.[6,29] While the nitride based devices which are currently commercially available can exhibit higher brightness and efficiency compared to the devices in this work, it should be noted that we do not use any kind of reactive ion etching which simplifies device fabrication. Also, the light extraction from the devices and the contact resistance is currently not optimized, so that further improvements can be expected with device optimization.

IV. CONCLUSIONS

In summary, ZnO/GaN based heterojunction LEDs were fabricated using a simple low-cost and low temperature electrodeposition method to obtain dense array of ZnO nanorods. The origin of different emission bands was studied for various p-GaN-based structures. It was found that all the emission bands (yellow-orange, blue, and violet) under both forward and reverse bias originated from p-GaN rather than ZnO. The yellow-orange emission likely originates from surface/interface defects, while violet emission likely originates from transitions involving acceptor levels in the p-GaN layer. While simple p-GaN/n-ZnO heterojunction devices exhibited relatively low brightness (tens of cd/m^2), devices incorporating InGaN MQWs exhibited considerably higher brightness. The brightest devices exhibited luminance exceeding 10 000 cd/m^2 at a bias of 30 mA.

ACKNOWLEDGMENTS

Financial support from the Strategic Research Theme, University Development Fund, and Seed Funding Grant, (administrated by The University of Hong Kong), Hung Hing Ying Physical Sciences Research Fund, and Innovation & Technology Fund Grant No. ITS/129/08 is acknowledged.

[1]A. B. Djurišić and Y. H. Leung, Small **2**, 944 (2006).
[2]X. M. Zhang, M. Y. Lu, Y. Zhang, L. J. Chen, and Z. L. Wang, Adv. Mater. **21**, 2767 (2009).
[3]E. Lai, W. Kim, and P D. Yang, Nano Res. **1**, 123 (2008).
[4]W. L. Park and G. C. Yi, Adv. Mater. **16**, 87 (2004).
[5]S.-D. Lee, Y.-S. Kim, M.-S. Yi, J.-Y. Choi, and S.-W. Kim, J. Phys. Chem. C **113**, 8954 (2009).

[6]D. J. Rogers, F. H. Teherani, A. Yasan, K. Minder, P. Kung, and M. Razeghi, Appl. Phys. Lett. **88**, 141918 (2006).
[7]M. C. Jeong, B. Y. Oh, M. H. Ham, and J. M. Myong, Appl. Phys. Lett. **88**, 202105 (2006).
[8]Q. Qin, L. W. Guo, Z. T. Zhou, H. Chen, X. L. Du, Z. X. Mei, J. F. Jia, Q. K. Xue, and J. M. Zhou, Chin. Phys. Lett. **22**, 2298 (2005).
[9]M. K. Wu, Y. T. Shih, W. C. Li, H. C. Chen, M. J. Chen, H. Kuan, J. R. Yang, and M. Shiojiri, IEEE Photon. Technol. Lett. **20**, 1772 (2008).
[10]A. M. C. Ng, Y. Y. Xi, Y. F. Hsu, A. B. Djurišić, W. K. Chan, S. Gwo, H. L. Tam, K. W. Cheah, P. W. K. Fong, H. F. Lui, and C. Surya, Nanotechnology **20**, 445201 (2009).
[11]I. E. Titkov, L. A. Delimova, A. S. Zubrilov, N. V. Seredova, I. A. Liniicuk, and I. V. Grekhov, J. Mod. Opt. **56**, 653 (2009).
[12]X. Y. Chen, A. M. C. Ng, F. Fang, A. B. Djurišić, W. K. Chan, H. L. Tam, K. W. Cheah, P. W. K. Fong, H. F. Lui, and C. Surya, J. Electrochem. Soc. **157**, H308 (2010).
[13]A. M. C. Ng, X. Y. Chen, F. Fang, Y. F. Hsu, A. B. Djurišić, C. C. Ling, H. L. Tam, K. W. Cheah, P. W. K. Fong, H. F. Lui, C. Surya, and W. K. Chan, Appl. Phys. B **100**, 851 (2010).
[14]J. W. Sun, Y. M. Lu, Y. C. Liu, D. Z. Shen, Z. Z. Zhang, B. H. Li, J. Y. Zhang, B. Yao, D. X. Zhao, and X. W. Fan, J. Phys. D: Appl. Phys. **41**, 155103 (2008).
[15]R. Guo, J. Nishimura, M. Matsumoto, M. Higashihata, D. Nakamura, and T. Okada, Appl. Phys. B **94**, 33 (2009).
[16]H. H. Huang, G. J. Fang, X. M. Mo, H. Long, L. Y. Yuan, B. Z. Dong, X. Q. Meng, and X. Z. Zhao, IEEE Electron Device Lett. **30**, 1063 (2009).
[17]C.-H. Chen, S.-J. Chang, S.-P. Chang, M.-J. Li, I. C. Chen, T.-J. Hsueh, and C.-L. Hsu, Appl. Phys. Lett. **95**, 223101 (2009).
[18]S.-H. Hwang, T.-H. Chung, and B.-T. Lee, Mater. Sci. Eng. B **157**, 32 (2009).
[19]G. Namkoong, E. Trybus, M. C. Cheung, W. A. Doolittle, A. N. Cartwright, I. Ferguson, T.-Y. Seong, and J. Nause, Appl. Phys. Express **3**, 022101 (2010).
[20]S. Dalui, C.-C. Lin, H.-Y. Lee, S.-F. Yen, Y.-J. Lee, and C.-T. Lee, J. Electrochem. Soc. **157**, H516 (2010).
[21]J. R. Sadaf, M. Q. Israr, S. Kishwar, O. Nur, and M. Willander, Nanoscale Res. Lett. **5**, 957 (2010).
[22]N. H. Alvi, M. Riaz, G. Tzamalis, O. Nur, and M. Willander, Semicond. Sci. Technol. **25**, 065004 (2010).
[23]D.-K. Hwang, S.-H. Kang, J.-H. Lim, E.-J. Yang, J.-Y. Oh, J.-H. Yang, and S.-J. Park, Appl. Phys. Lett. **86**, 222101 (2005).
[24]O. Lupan, T. Pauporté, and B. Viana, Adv. Mater. **22**, 3298 (2010).
[25]R. W. Chuang, R.-W. Wu, L.-W. Lai, and C.-T. Lee, Appl. Phys. Lett. **91**, 231113 (2007).
[26]J. Y. Lee, J. H. Lee, H. S. Kim, C.-H. Lee, H.-S. Ahn, H. K. Cho, Y. Y. Kim, B. H. Kong, and H. S. Lee, Thin Solid Films **517**, 5157 (2009).
[27]H.-C. Chen, M.-J. Chen, M.-K. Wu, W.-C. Li, H.-L. Tsai, J.-R. Yang, H. Kuan, and M. Shiojiri, IEEE J. Quantum Electron. **46**, 265 (2010).
[28]J. R. Sadaf, M. Q. Israr, S. Kishwar, O. Nur, and M. Willander, Semicond. Sci. Technol. **26**, 075003 (2011).
[29]M. J. Chen, Y.-T. Shih, M.-K. Wu, H.-C. Chen, H.-L. Tsai, W.-C. Li, J.-R. Yang, H. Kuan, and M. Shiojiri, IEEE Trans. Electron Devices **57**, 2195 (2010).
[30]H. Gao, F. Yan, J. Li, Y. Zeng, and J. Wang, J. Phys. D: Appl. Phys. **40**, 3654 (2007).
[31]C. Bayram, F. H. Teherani, D. J. Rogers, and M. Razeghi, Appl. Phys. Lett. **93**, 081111 (2008).
[32]C. Bayram, M. Razeghi, D. J. Rogers, and F. H. Teherani, J. Vac. Sci. Technol. **27**, 1784 (2009).
[33]C.-H. Lee, J. Yoo, Y. J. Hong, J. Cho, Y.-J. Kim, S.-R. Jeon, J. H. Baek, and G.-C. Yi, Appl. Phys. Lett. **94**, 213101 (2009).
[34]I. Mora-Seró, F. Fabregat-Santiago, B. Denier, J. Bisquert, R. Tena-Zaera, J. Elias, and C. Lévy-Clément, Appl. Phys. Lett. **89**, 203117 (2006).
[35]R. Dimitrova, L. Catalan, D. Alexandrov, and A. Chen, Electroanalysis **20**, 789 (2008).
[36]B.-Y. Chang and S.-M. Park, Annu. Rev. Anal. Chem. **3**, 207 (2010).
[37]See supplementary material at http://dx.doi.org/10.1063/1.3653835 for detailed characterization results for all the devices.
[38]A. Hepp, H. Heil, W. Weise, M. Ahles, R. Schmechel, and H. von Seggern, Phys. Rev. Lett. **91**, 157406 (2003).
[39]I. Pang, H. Kim, S. Kim, K. Jeong, H. S. Jung, C. J. Yu, H. Soh, and J. Lee, Org. Electron. **11**, 338 (2010).
[40]M. Muccini, Nature Mater **5**, 605 (2006).
[41]K. K. Ng and S. M. Sze, *Physics of Semiconductor Devices* (Wiley, New York, 2007).
[42]Y. G. Cao, L. Miao, S. Tanemura, M. Tanemura, Y. Kuno, and Y. Hayashi, Appl. Phys. Lett. **88**, 251116 (2006).
[43]P. L. Chen, X. Y. Ma, and D. R. Yang, J. Appl. Phys. **101**, 053103 (2007).
[44]A. B. Djurišić, Y. H. Leung, K. H. Tam, Y. F. Hsu, L. Ding, W. K. Ge, Y. C. Zhong, K. W. Wong, W. K. Chan, H. L. Tam, K. W. Cheah, W. M. Kwok, and D. L. Phillips, Nanotechnology **18**, 095702 (2007).
[45]T. Nakayama and M. Murayama, J. Cryst. Growth **214/215**, 299 (2000).
[46]H. F. Liu, G. X. Hu, H. Gong, K. Y. Zang, and S. J. Chua, J. Vac. Sci. Technol. A **26**, 1462 (2008).
[47]S. K. Hong, T. Hanada, H. Makino, H. J. Ko, Y. Chen, T. Yao, A. Tanaka, H. Sasaki, S. Sato, D. Imai, K. Araki, and M. Shinohara, J. Vac. Sci. Technol. B **19**, 1429 (2001).
[48]M. F. Schubert, Phys. Rev. B **81**, 035303 (2010).
[49]V. E. Kudryashov and A. É. Yunovich, J. Exp. Theor. Phys. **97**, 1015 (2003).
[50]M. A. Zimmler, J. M. Bao, I. Shalish, W. Yi, V. Narayanamurti, and F. Capasso, Nanotechnology **18**, 395201 (2007).
[51]M. A. Zimmler, J. M. Bao, I. Shalish, W. Yi, J. Yoon, V. Narayanamurti, and F. Capasso, Nanotechnology **18**, 235205 (2007).
[52]A. L. Milnes and D. L. Feucht, *Heterojunctions and Metal-Semiconductor Junctions* (Academic, New York, 1972).
[53]A. Hierro, D. Kwon, S. A. Ringel, M. Hansen, J. S. Speck, U. K. Mishra, and S. P. DenBaars, Appl. Phys. Lett. **76**, 3064 (2000).
[54]N. I. Bochkareva, V. V. Voronenkov, R. I. Gorbunov, A. S. Zubrilov, Y. S. Lelikov, F. E. Latyshev, Y. T. Rebane, A. I. Tsyuk, and Y. G. Shreter, Semiconductors **44**, 794 (2010).
[55]J.-L. Lee, J. K. Kim, J. W. Lee, Y. J. Park, and T. Kim, Phys. Status Solidi A **176**, 763 (1999).